# Supplemental Materials

## Prediction of Carboxylesterase 1 (CES1)-mediated *In Vivo* Drug Interaction between Methylphenidate and Cannabinoids using Static and Physiologically Based Pharmacokinetic Models

Yuli Qian, Ph.D. and John S. Markowitz, Pharm.D.

Department of Pharmacotherapy and Translational Research, College of Pharmacy, University of Florida, Gainesville, Florida, USA

**Appendix A.** Derivation of THC and CBD binding in the incubation mixture in the presence of protein

At equilibrium, the binding of cannabinoid to tube wall and protein can be described below:

$$[S] \cdot [W] \cdot K_w = SW_p \quad \text{(S1)}$$

$$[S] \cdot [P] \cdot K_p = SP \quad \text{(S2)}$$

where [S] is the unbound cannabinoid concentration, [W] is wall available for cannabinoid binding, $SW_p$ is the cannabinoid bound to tube wall at the presence of protein, [P] is the protein available for cannabinoid binding, SP is the cannabinoid bound to protein, $K_w$ represents the binding constant between cannabinoid and tube wall, and $K_p$ represents the binding constant between cannabinoid and protein.

Since the total cannabinoid in the system ($S_T$) equals to the sum all forms of cannabinoid (i.e. [S]+$SW_p$+SP), Equation S2 can be re-written to:

$$[S] \cdot \left(1 + K_p \cdot [P]\right) = S_T - SW_p \quad \text{(S3)}$$

Further replace [S] by combining S1 and S3:

$$\frac{SW_p}{K_w \cdot [W]} \cdot \left(1 + K_p \cdot [P]\right) = S_T - SW_p \quad \text{(S4)}$$

Similarly, the total tube wall available for cannabinoid binding ($W_T$) equals the sum of [W] and $SW_p$, and Equation S4 can be re-written as:

$$\frac{SW_p}{K_w \cdot (W_T - SW_p)} \cdot \left(1 + K_p \cdot [P]\right) = S_T - SW_p \quad \text{(S5)}$$

The equation can be further arranged into the form below:

$$SW_p{}^2 - \left(S_T + W_T + \frac{1 + K_p \cdot [P]}{K_w}\right) \cdot SW_p + S_T \cdot W_T = 0 \quad \text{(S6)}$$

This quadratic equation can be solved, and the real solution is as follows:

$$SW_p = \frac{\left(S_T + W_T + \frac{K_p \cdot [P]}{K_w} + \frac{1}{K_w}\right) - \sqrt{\left(S_T + W_T + \frac{K_p \cdot [P]}{K_w} + \frac{1}{K_w}\right)^2 - 4W_T \cdot S_T}}{2} \quad \text{(S7)}$$

**Appendix B.** Back-calculation of Intrinsic Clearance of CBD

The fraction of CBD metabolized ($f_m$) by CYP3A4 (0.54), CYP2C19 (0.31), and CYP2C9 (0.15) were obtained from an in vitro CBD depletion assay (Beers et al., 2021).

The value of $f_m$ for CYP3A4 was further supported by a clinical study where an oromucosal spray of THC/CBD was co-administered with ketoconazole, a strong clinical inhibitor of CYP3A4/5 (Stott et al., 2013). By assuming complete inhibition of CYP3A4-mediated CBD metabolism, the $f_m$ of CBD by CYP3A4 was calculated as follows:

$$f_{m,3A4} = 1 - \frac{AUC_{alone}}{AUC_i} \quad \text{(S8)}$$

where $AUC_{alone}$ represents the AUC of CBD when dosed without ketoconazole (3.54 ng·hr/ml), and $AUC_i$ represents the AUC of CBD when co-administered with ketoconazole (6.50 ng·hr/ml). The resulting $f_m$ for CYP3A4 is 0.46.

The hepatic plasma clearance ($CL_{H,plasma}$) of CBD was observed after intravenous administration and reported as 74.4 L/hr (Ohlsson et al., 1986). The total intrinsic hepatic clearance ($CL_{int,H}$) was then back-calculated using the following equation:

$$CL_{int,H} = \frac{Q_{H,B} \times CL_{H,plasma}}{f_u \times (Q_{H,B} - CL_{H,plasma}/(B:P))} \quad \text{(S9)}$$

$Q_{H,B}$ represents hepatic blood flow, and its value (99 L/hr) was obtained from PK-Sim® simulated individual with demographics matching the ones in the study by Ohlsson et al. fu is the unbound fraction of CBD and a value of 0.06 was used (Epidiolex® NDA). The blood-to-plasma drug concentration ratio (B:P) was assumed to be 1 due to lack of

data availability. This assumption was supported by a similar B:P value (1.03) predicted by the software in the final model.

The resulting $CL_{int,H}$ value (4990 L/hr) was further converted to intrinsic clearance of individual enzymes as follows:

$$CL_{int,enzyme} = \frac{CL_{int,H} \times f_m}{C_{enzyme} \times V_H \times 60} \quad \text{(S10)}$$

where $f_m$ is the fraction of CBD metabolized by individual enzymes, $C_{enzyme}$ is the concentration of individual enzyme in the liver, and $V_H$ is the liver volume. Values of $f_m$ (0.54 for CYP3A4, 0.31 for CYP2C19, and 0.15 for CYP2C9) were inferred from clinical study as described below. $C_{enzyme}$ (4.32 µmol/L liver for CYP3A4, 0.76 µmol/L liver for CYP2C19, and 3.84 µmol/L liver for CYP2C9) were default values in PK-Sim® database and $V_H$ (2.25 L) was obtained from simulated individual with demographics matching the ones in the study by Ohlsson et al. The numeric value of 60 was utilized for unit conversion (i.e. “µl/hr/pmol protein” to “µl/min/pmol protein”). The demographics of subjects from the Ohlsson study are provided in Supplemental Table 3.

The calculated $CL_{int,3A4}$, $CL_{int,2C19}$, and $CL_{int,2C9}$ are 4.62, 15.1, and 1.44 µl/min/pmol protein, respectively.

**Supplemental Table 1.** Linearity, accuracy, and intraday and interday precision of RA, THC, and CBD.

| | Analyte level[a] | Day 1 | Day 2 | Day 3 | CV (%, interday) |
|---|---|---|---|---|---|
| **RA[b]** | | | | | |
| Mean (accuracy) | 5 | 4.9 (97%) | 5.0 (101%) | 4.9 (97%) | 1.9 |
| CV (%, intraday) | | 16.1 | 10.4 | 2.7 | |
| Mean (accuracy) | 10 | 10.5 (105%) | 9.9 (99%) | 10.6 (106%) | 3.4 |
| CV (%, intraday) | | 1.5 | 13.7 | 1.6 | |
| Mean (accuracy) | 100 | 99.8 (100%) | 109 (109%) | 98.6 (99%) | 5.6 |
| CV (%, intraday) | | 10.9 | 2.1 | 4.7 | |
| **THC[c]** | | | | | |
| Mean (accuracy) | 25 | 24.6 (98%) | 25.3 (101%) | 24.9 (100%) | 1.4 |
| CV (%, intraday) | | 6.1 | 8.0 | 1.2 | |
| Mean (accuracy) | 50 | 51.2 (102%) | 45.8 (92%) | 49.4 (99%) | 5.6 |
| CV (%, intraday) | | 0.8 | 4.9 | 6.9 | |
| Mean (accuracy) | 200 | 189 (94%) | 215 (107%) | 195 (98%) | 6.8 |
| CV (%, intraday) | | 5.4 | 8.0 | 0.6 | |
| **CBD[d]** | | | | | |
| Mean (accuracy) | 25 | 24.5 (98%) | 25.9 (104%) | 24.7 (99%) | 3.1 |
| CV (%, intraday) | | 7.8 | 15.8 | 6.1 | |
| Mean (accuracy) | 50 | 52.1 (104%) | 46.7 (93%) | 50.9 (102%) | 5.7 |
| CV (%, intraday) | | 3.4 | 17.8 | 1.5 | |
| Mean (accuracy) | 200 | 194 (97%) | 203 (102%) | 185 (92%) | 4.8 |
| CV (%, intraday) | | 7.2 | 6.9 | 1.9 | |

RA, ritalinic acid; THC, $\Delta^9$-tetrahydrocannabinol; CBD, cannabidiol; CV, coefficient of variation.

[a] Values shown in nM for RA and ng/ml for THC and CBD.

[b] Linear range of calibration standards: 5 – 500 nM with a mean correlation coefficient of 0.991.

[c] Linear range of calibration standards: 25 – 400 ng/ml with a mean correlation coefficient of 0.990.

[d] Linear range of calibration standards: 25 – 400 ng/ml with a mean correlation coefficient of 0.987.

**Supplemental Table 2.** Demographics of subjects in the MPH studies used for model development and verification.

| Study | N (%female) | Age (SD) | Body weight (SD) | Drug administration |
|---|---|---|---|---|
| (Srinivas et al., 1993) | 13 (0) | 18-30[a] | NA | 10 mg racemic MPH (intravenous) |
| (Midha et al., 2001) | 24 (0) | 18-50[a] | NA | 40 mg Ritalin® |
| (Patrick et al., 2007) | 20 (53) | M: 28.8 (5.3)<br>F: 28.7 (4.4) | M: 82.2 (10.5)<br>F: 65.2 (8.4) | 0.3 mg/kg Ritalin® |
| (Spencer et al., 2006) | 12 (50) | 24 (2.4) | NA | 40 mg Ritalin® |
| (Teo et al., 2004) | 15 (40) | 30 (20-44)[a] | 72 (54-100)[a] | 20 mg Focalin® |
| (Wong et al., 1998) | 22 (0) | 27.6 (6.1) | 74.7 (9) | 40 mg Ritalin® |
| (Patrick et al., 2013) | 24 (50) | M: 25.8 (2.4)<br>F: 26.9 (4.5) | M: 82.2 (11.1)<br>F: 59.6 (6.8) | 0.3 mg/kg Ritalin® |
| (Parasrampuria et al., 2007) | 49 (NA) | 18-45[a] | NA | 50 and 90 mg Ritalin® |
| (Hysek et al., 2014) | 16 (50) | 24.8 (2.6) | 66.7 | 60 mg Ritalin® |
| (Abbas et al., 2016) | 31 (52) | 32 (10) | 72.6 (10.9) | 40 mg Ritalin® at 0 and 6 hour |
| (Adjei et al., 2014) | 26 (42) | 27.8 (7.3) | 70.4 (11.7) | 25 mg Ritalin® at 0, 4, and 8 hour |
| (DeVane et al., 2000) | 6 (17) | 18-55 | NA | 10 mg Ritalin® |
| (Koehm et al., 2010) | 10 (0) | 26 (20-40)[a] | NA | 20 mg Ritalin® |
| (Meyer et al., 2000) | 20 (0) | 20-33[a] | NA | 20 mg Ritalin® |
| (Patrick et al., 1989) | 18 (0) | NA | NA | 10 mg Ritalin® at 0 and 5 hour |
| (Spencer et al., 2012) | 26 (NA) | 18-55[a] | NA | 40 mg Ritalin® at 0 and 4 hour |
| (Stage et al., 2017) | 16 (50) | 24 (21-29)[a] | 66.5 (54.5-104)[a] | 10 mg Ritalin® |

N, number of subjects. SD, standard deviation. NA, value not reported; MPH, methylphenidate.

[a] Range values reported.

**Supplemental Table 3.** Demographics of subjects in the CBD studies used for model development and verification.

| Study | N (%female) | Age (SD) | Body weight (SD) | Drug administration |
|---|---|---|---|---|
| (Ohlsson et al., 1986) | 5 (0) | 26.4 (19-33)[a] | 78.6 (66-93)[a] | 20 mg CBD (intravenous) |
| (Taylor et al., 2018) | 6 (83) | 26 (3.2) | NA | 1500 mg Epidiolex® |
| (Taylor et al., 2018) | 6 (50) | 25 (4.7) | NA | 3000 mg Epidiolex® |
| (Taylor et al., 2018) | 6 (100) | 25.8 (7.9) | NA | 4500 mg Epidiolex® |
| (Taylor et al., 2018) | 6 (67) | 22.8 (3.2) | NA | 6000 mg Epidiolex® |
| (Crockett et al., 2020) | 29 (59) | 36.6 (14.3) | 71.7 (11.0) | 750 mg Epidiolex® |
| (Taylor et al., 2019) | 8 (50) | 55 (10) | 89.4 (11.6) | 200 mg Epidiolex® |
| (Tayo et al., 2020) | 8 (63) | 60.4 (11.5) | NA | 200 mg Epidiolex® |

N, number of subjects. SD, standard deviation. NA, value not reported; CBD, cannabidiol.

[a] Range values reported.

**Supplemental Table 4.** Drug-specific input parameters for MPH model.

| Parameter | Unit | Value | Source |
|---|---|---|---|
| Molecular weight | g/mol | 233.3 | - |
| Lipophilicity | - | 2.02 | Predicted[c] |
| pKa (base) | - | 8.9 | The Merck Index |
| $f_u$ | - | 0.84 | (Hungund et al., 1979) |
| FaSSIF solubility | mg/ml | 6.04 | Predicted[c] |
| FeSSIF solubility | mg/ml | 8.70 | Predicted[c] |
| Intestinal permeability | cm/min | $3.69\times10^{-5}$ | Predicted[d] |
| **Metabolism** | | | |
| CES1 $K_m$ (d-MPH) | µM | 118.3 | (Sun et al., 2004) |
| CES1 $V_{max}$ (d-MPH) | pmol/min/pmol enzyme | 2.26 | Optimized |
| CES1 $K_m$ (l-MPH) | µM | 43.6 | (Sun et al., 2004) |
| CES1 $V_{max}$ (l-MPH) | pmol/min/pmol enzyme | 22.4 | Optimized |
| Non-CES1 $CL_{int}$ (d-MPH)[a] | µl/min/pmol enzyme | 0.0048 | Optimized |
| Non-CES1 $CL_{int}$ (l-MPH)[a] | µl/min/pmol enzyme | 0.129 | Optimized |
| **Interactions** | | | |
| $K_i$ on CES1 (d-MPH)[b] | µM | 118.3 | (Sun et al., 2004) |
| $K_i$ on CES1 (l-MPH)[b] | µM | 43.6 | (Sun et al., 2004) |
| **Formulation** | | | |
| 50% dissolution time | hr | 1.03 | Optimized |
| Lag time | hr | 0 | Fixed |
| Shape factor | - | 1.31 | Fixed[e] |

MPH, methylphenidate; pKa, acid dissociation constant; fu, fraction unbound; FaSSIF, fasted state simulated intestinal fluid; FeSSIF, fed state simulated intestinal fluid; CES1, carboxylesterase 1; $K_m$, Michaelis-Menten constant; $V_{max}$, maximum rate of reaction; $CL_{int}$, intrinsic clearance; $K_i$, inhibition constant.

[a] Manually adjusted to account for 20% of MPH metabolism (Faraj et al., 1974).

[b] Competitive interactions assumed between two enantiomers to the binding site of CES1.

[c] From ADMET Predictor v9.5.0.

[d] From PK-Sim v9.1.

[e] Estimated from literature data (Wang et al., 2004).

**Supplemental Table 5.** Drug-specific input parameters for CBD model.

| Parameter | Unit | Value | Source |
|---|---|---|---|
| Molecular weight | g/mol | 314.5 | - |
| Lipophilicity | - | 3.15 | Optimized |
| pKa (acid) | - | 9.7, 10.8 | Predicted[a] |
| $f_u$ | - | 0.06 | Epidiolex® NDA |
| FaSSIF solubility | µg/ml | 10.7 | (Bansal et al., 2020) |
| FeSSIF solubility | µg/ml | 12.6 | (Bansal et al., 2020) |
| Intestinal permeability | cm/min | $3.41\times10^{-4}$ | Optimized |
| **Metabolism** | | | |
| CYP3A4 $CL_{int}$ | µl/min/pmol enzyme | 4.62 | Back-calculated[b] |
| CYP2C19 $CL_{int}$ | µl/min/pmol enzyme | 15.1 | Back-calculated[b] |
| CYP2C9 $CL_{int}$ | µl/min/pmol enzyme | 1.44 | Back-calculated[b] |
| **Interactions** | | | |
| $K_{i,u}$ on CES1 | µM | 0.091 | In-house |
| $K_{I,u}$ on CYP3A4 | µM | 0.58 | (Bansal et al., 2020) |
| $k_{inact}$ on CYP3A4 | /min | 0.08 | (Bansal et al., 2020) |
| $K_{I,u}$ on CYP2C19 | µM | 0.40 | (Bansal et al., 2020) |
| $k_{inact}$ on CYP2C19 | /min | 0.04 | (Bansal et al., 2020) |
| $K_{i,u}$ on CYP2C9 | µM | 0.17[c] | (Bansal et al., 2020) |
| **Formulation** | | | |
| 50% dissolution time (Weibull 1) | hr | 1.42 | Optimized |
| Lag time (Weibull 1) | hr | 0 | Fixed |
| Shape factor (Weibull 1) | - | 3.01 | Optimized |
| Delay factor (Weibull 1) | - | 0.81 | Optimized |
| 50% dissolution time (Weibull 2) | hr | 2.92 | Optimized |
| Lag time (Weibull 2) | hr | 1.00 | Optimized |
| Shape factor (Weibull 2) | - | 3.51 | Optimized |
| Delay factor (Weibull 2) | - | 0.47 | Optimized |

CBD, cannabidiol; pKa, acid dissociation constant; fu, fraction unbound; FaSSIF, fasted state simulated intestinal fluid; FeSSIF, fed state simulated intestinal fluid; CES1, carboxylesterase 1; $CL_{int}$, intrinsic clearance; $K_{i,u}$, unbound inhibition constant; $K_{I,u}$, unbound inhibitor concentration achieving 50% $k_{inact}$; $k_{inact}$, maximum inactivation rate constant.

[a] From ADMET Predictor v9.5.0.

[b] Calculated based on well-stirred model and fraction of clearance of 0.46 and 0.54 for CYP3A4 and CYP2C19, respectively.

[c] $IC_{50,u}$ value reported by Bansal et al. used as $K_{i,u}$.

**Supplemental Table 6.** Unbound concentrations of THC and CBD in the incubation mixture.

| **Cannabinoids added (μM)** | **Unbound (μM)** | **$f_{u,inc}$** |
|---|---|---|
| **THC** | | |
| 1.59 | 0.0233 | 0.0146 |
| 3.18 | 0.0467 | 0.0147 |
| 6.36 | 0.0940 | 0.0148 |
| 9.54 | 0.142 | 0.0149 |
| 15.9 | 0.239 | 0.0150 |
| 19.1 | 0.288 | 0.0151 |
| 31.8 | 0.487 | 0.0153 |
| | | |
| **CBD** | | |
| 1.59 | 0.0640 | 0.0403 |
| 3.18 | 0.129 | 0.0407 |
| 6.36 | 0.265 | 0.0416 |
| 12.7 | 0.550 | 0.0432 |
| 15.9 | 0.698 | 0.0439 |
| 25.4 | 1.16 | 0.0458 |
| 31.8 | 1.49 | 0.0468 |

THC, $\Delta^9$-tetrahydrocannabinol; CBD, cannabidiol; $f_{u,inc}$, unbound fraction of cannabinoid in the incubation mixture.

**Supplemental Figure 1.** Binding model of THC and CBD.

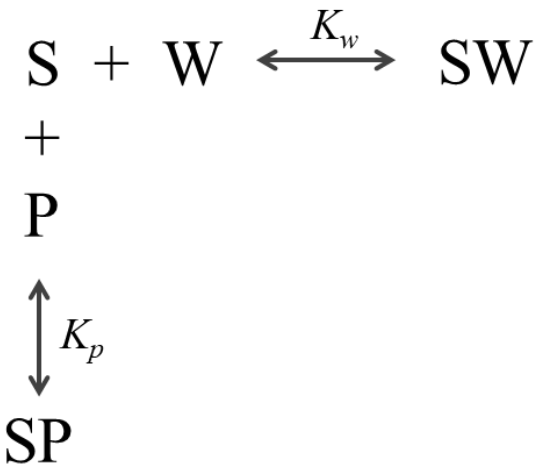


Cannabinoid (S) can bind nonspecifically to either the tube wall (W) or protein (P) in the incubation mixture. SW and SP are the cannabinoid-tube wall and cannabinoid-protein binding complexes, respectively. $K_w$ and $K_p$ are binding constants described in Equation 4 and 5. THC, $\Delta^9$-tetrahydrocannabinol; CBD, cannabidiol.

**Supplemental Figure 2.** Chromatograms of RA (red in panel A), THC (red in panel B) and CBD (red in panel C). Phenacetin (blue) was utilized as the internal standard.

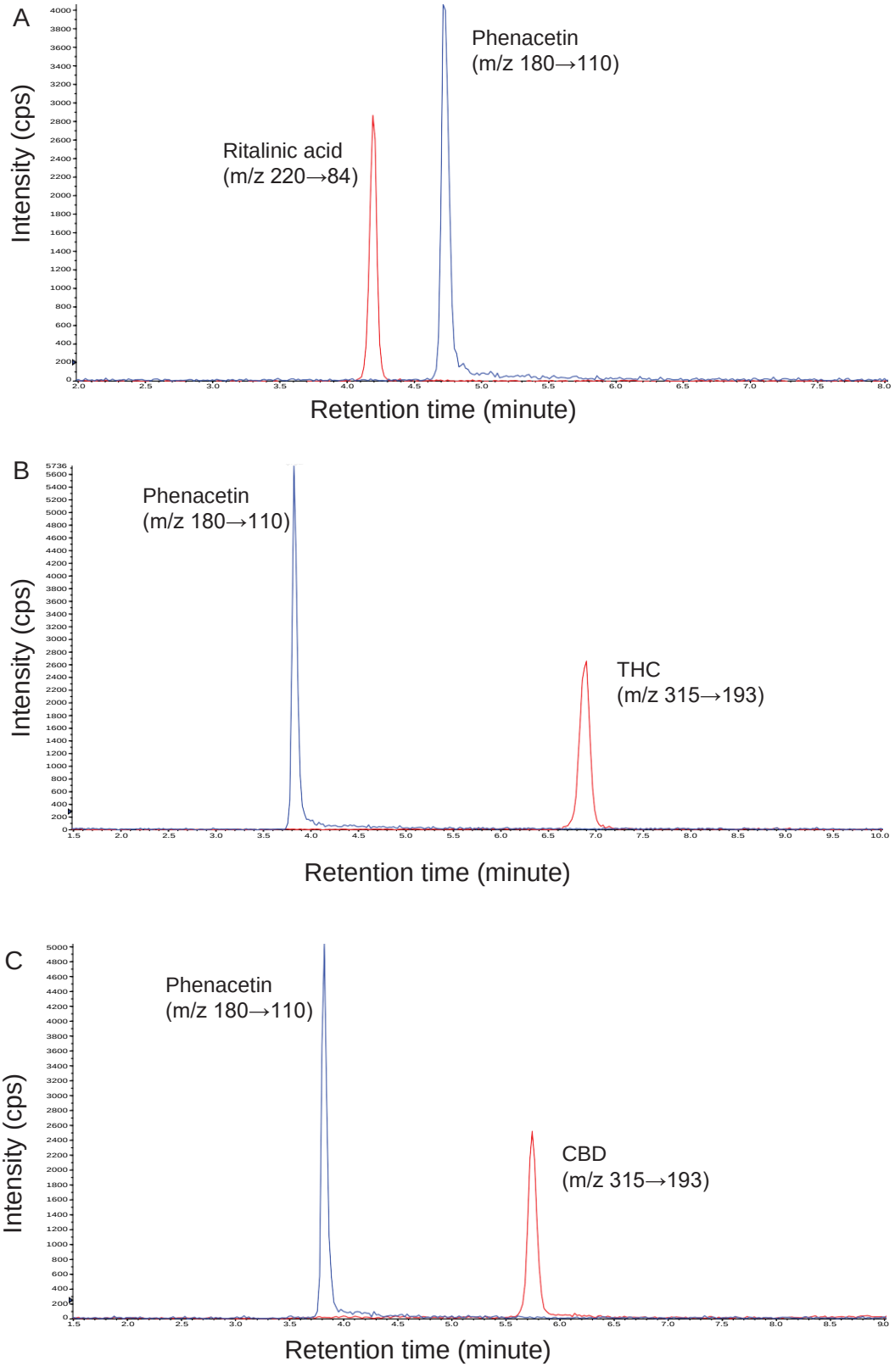

Analytes were separated on an HPLC column (50 × 2.0 mm, 5 µm C18) with a gradient mobile phase comprising water with 0.1% formic acid as the aqueous phase and methanol as the organic phase. Analytes were detected by a mass spectrometry operated in positive mode and with electrospray as the ionization method. The monitored mass transitions for RA, THC, CBD, and the internal standard phenacetin were m/z 220 → 84, 315 → 193, 315 → 193, and 180 → 110, respectively. RA, ritalinic acid; THC, $\Delta^9$-tetrahydrocannabinol; CBD, cannabidiol.

**Supplemental Figure 3.** A workflow of PBPK model development and verification for MPH and CBD and prediction of drug-drug interactions by simulation.

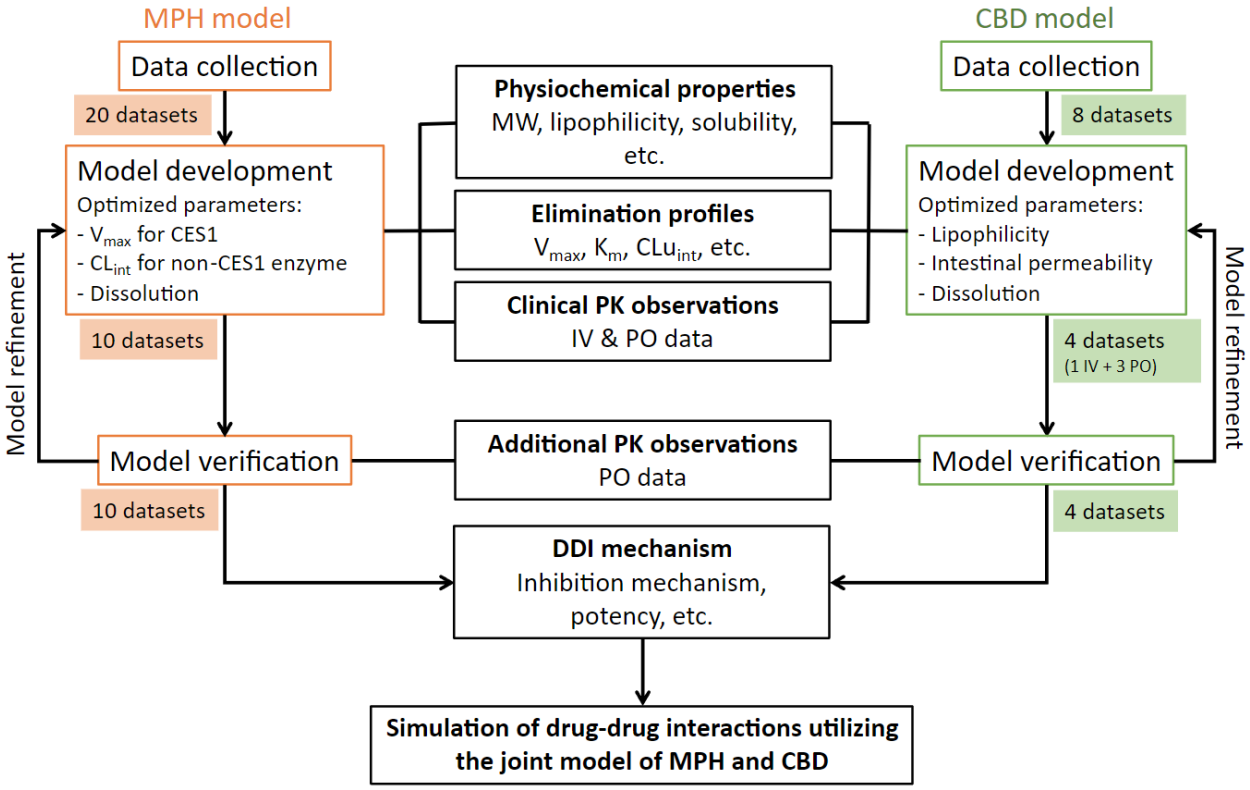

**Supplemental Figure 4.** Terminal half-lives of MPH reported in studies found from literature review.

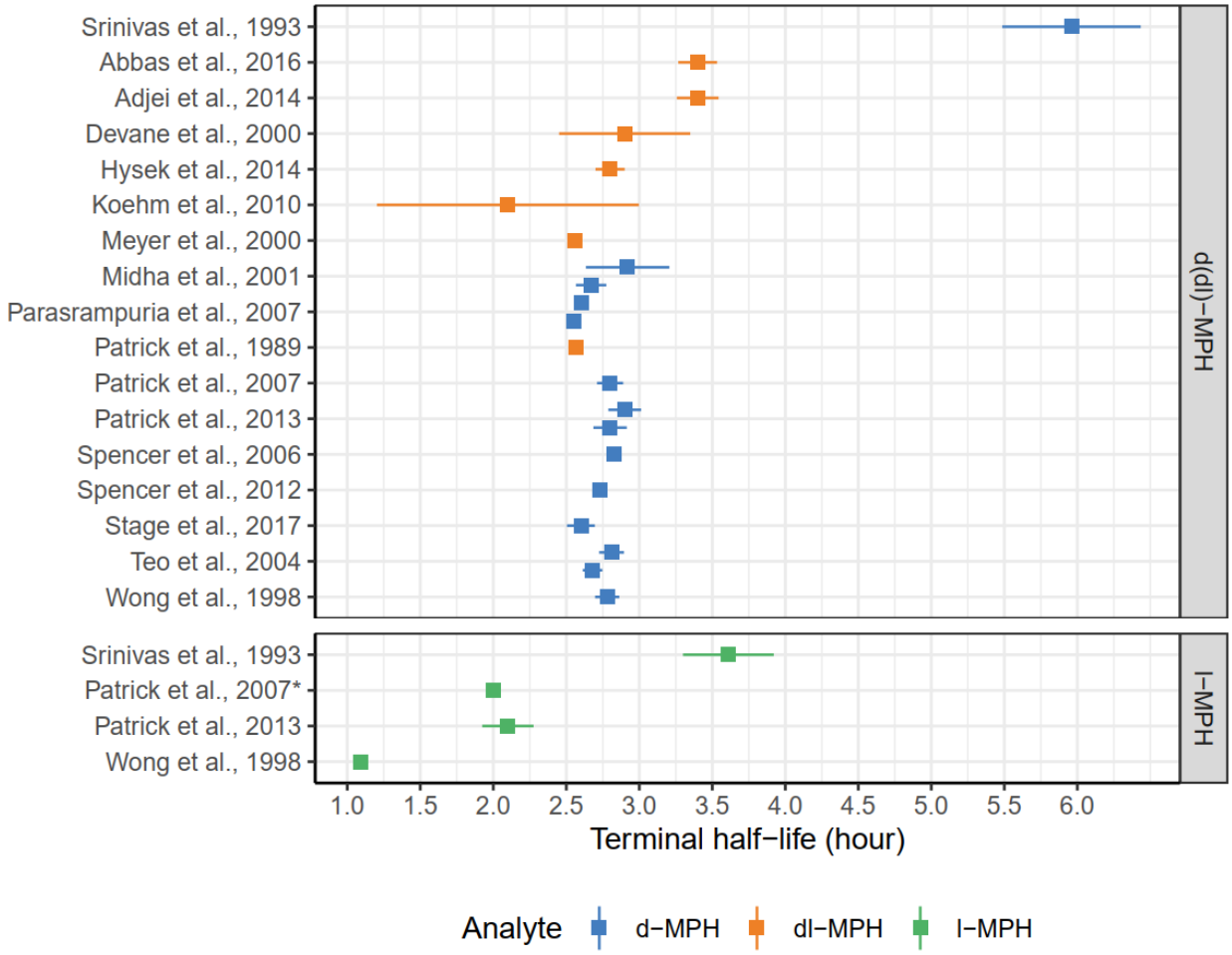


Points represented reported values of MPH terminal half-lives and their standard error. *d*-MPH was pooled with *dl*-MPH due to the predominant presence of the *d*-enantiomers in total MPH measured in plasma. Srinivas et al., 1993 is the only study with intravenous route of administration. MPH, methylphenidate.

* Half-life calculated from digitized population-level data.

**Supplemental Figure 5.** Sensitivity analysis to assess the parameters that impact CBD disposition after intravenous administration.

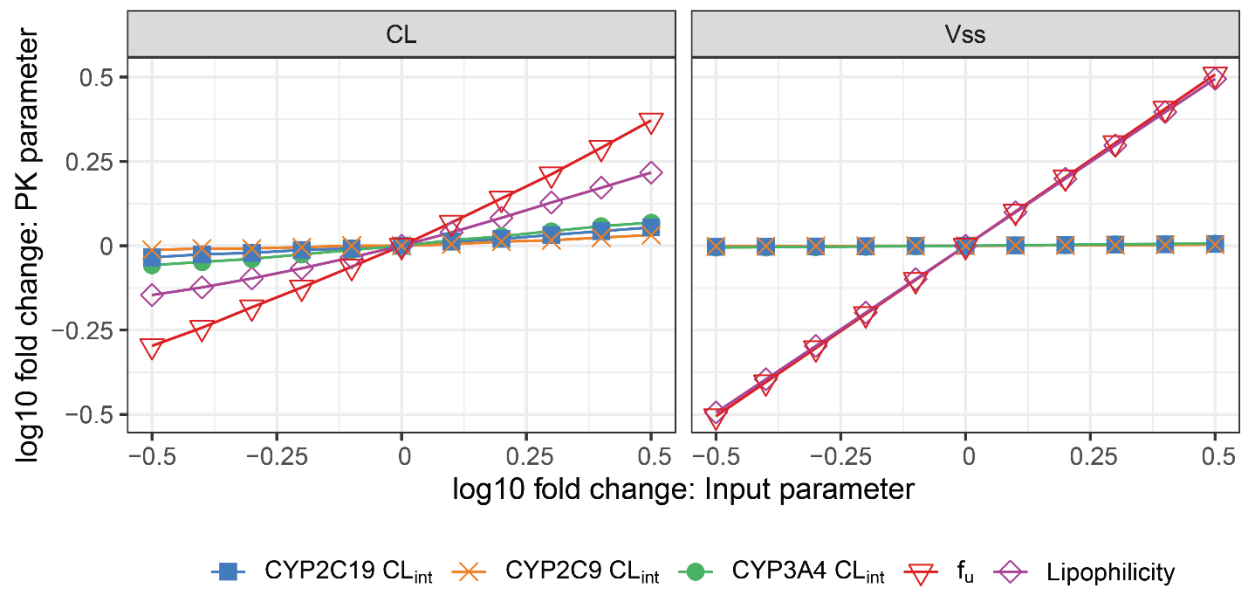


Lipophilicity and $f_u$ were found as the parameters exerting high impact on disposition of CBD. Due to identifiability issue, they were optimized separately by fitting the model into observed *in vivo* concentration-time profiles of CBD after intravenous administration. Optimization of lipophilicity rendered better goodness-of-fit and the estimated value (3.15) was utilized as the final parameter. Literature-reported value of $f_u$ (0.06) was used without any refinement. CBD, cannabidiol; CL, *in vivo* clearance; $V_{ss}$, volume of distribution at steady state.

**Supplemental Figure 6.** PBPK model simulated and observed concentration-time profiles of CBD after intravenous administration.

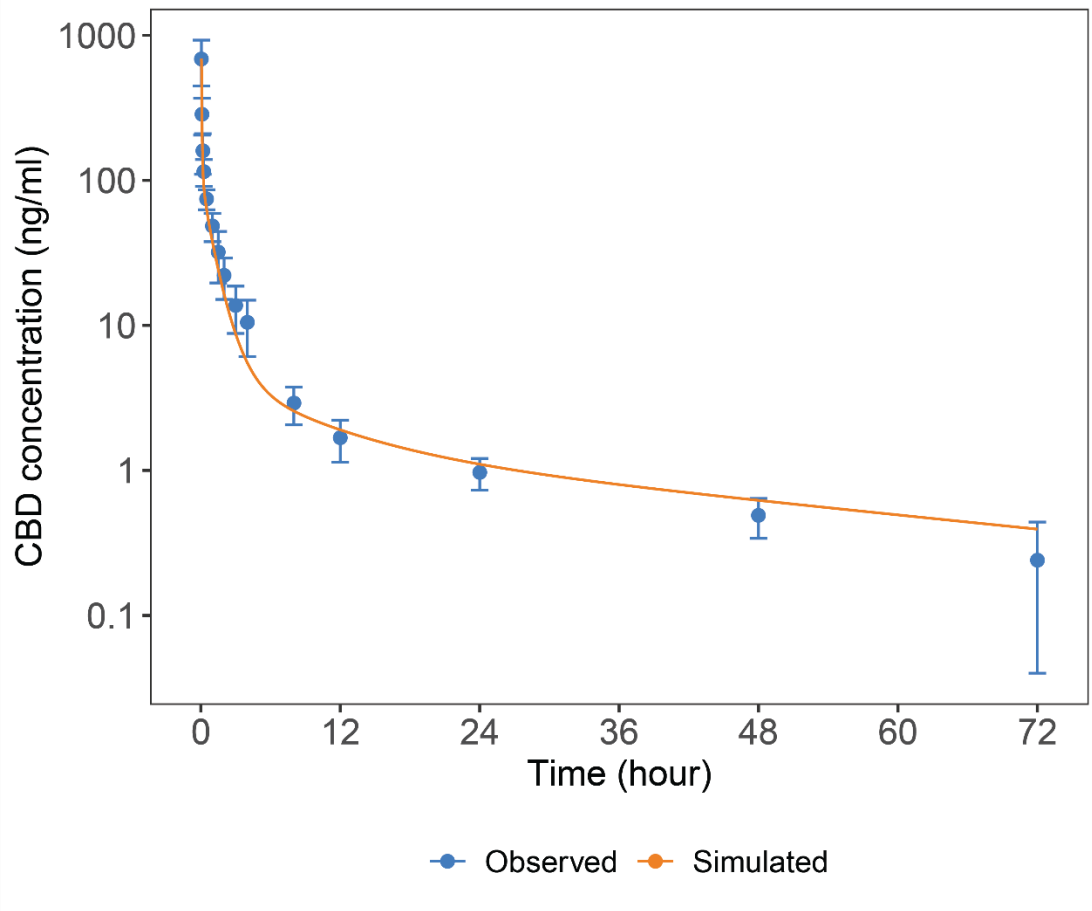


Lipophilicity of CBD was optimized by fitting the model into observed data after intravenous administration.

**Supplemental Figure 7.** Nonspecific binding of THC and CBD in the incubation mixture.

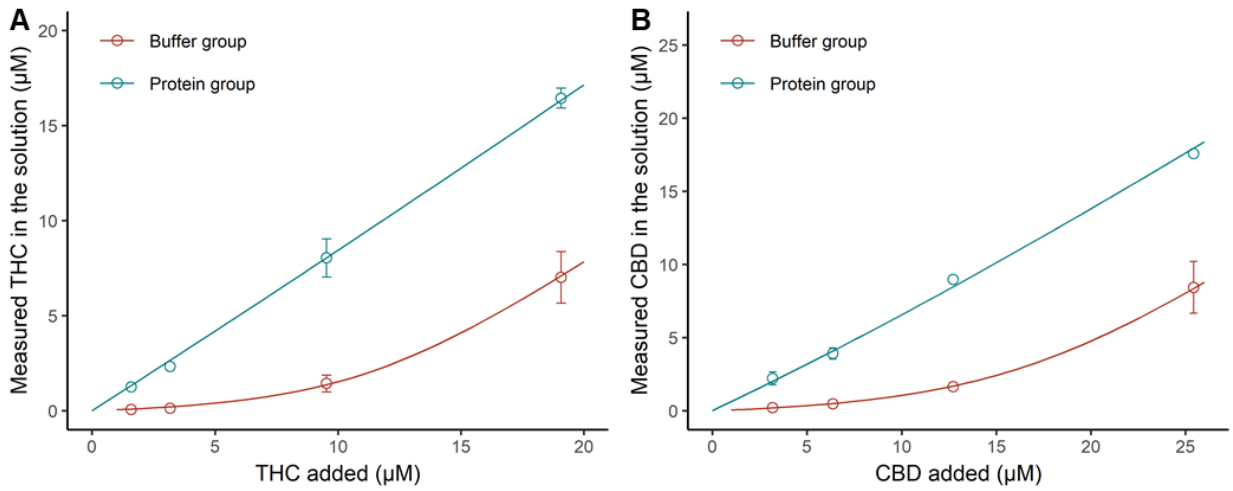


Cannabinoids were added into the mixture at the presence and absence of protein (BSA and HLS9). Data points represent the mean (±SD) of three independent experiments. Lines represent model prediction. THC, $\Delta^9$-tetrahydrocannabinol; CBD, cannabidiol.

## Reference


Abbas R, Palumbo D, Walters F, Belden H, and Berry SA (2016) Single-dose Pharmacokinetic Properties and Relative Bioavailability of a Novel Methylphenidate Extended-release Chewable Tablet Compared With Immediate-release Methylphenidate Chewable Tablet. *Clin Ther* 38**:**1151-1157.

Adjei A, Teuscher NS, Kupper RJ, Chang WW, Greenhill L, Newcorn JH, Connor DF, and Wigal S (2014) Single-dose pharmacokinetics of methylphenidate extended-release multiple layer beads administered as intact capsule or sprinkles versus methylphenidate immediate-release tablets (Ritalin((R))) in healthy adult volunteers. *J Child Adolesc Psychopharmacol* 24**:**570-578.

Bansal S, Maharao N, Paine MF, and Unadkat JD (2020) Predicting the Potential for Cannabinoids to Precipitate Pharmacokinetic Drug Interactions via Reversible Inhibition or Inactivation of Major Cytochromes P450. *Drug Metab Dispos* 48**:**1008-1017.

Beers JL, Fu D, and Jackson KD (2021) Cytochrome P450-Catalyzed Metabolism of Cannabidiol to the Active Metabolite 7-Hydroxy-Cannabidiol. *Drug Metab Dispos* 49**:**882-891.

Crockett J, Critchley D, Tayo B, Berwaerts J, and Morrison G (2020) A phase 1, randomized, pharmacokinetic trial of the effect of different meal compositions, whole milk, and alcohol on cannabidiol exposure and safety in healthy subjects. *Epilepsia* 61**:**267-277.

DeVane CL, Markowitz JS, Carson SW, Boulton DW, Gill HS, Nahas Z, and Risch SC (2000) Single-dose pharmacokinetics of methylphenidate in CYP2D6 extensive and poor metabolizers. *J Clin Psychopharmacol* 20**:**347-349.

Faraj BA, Israili ZH, Perel JM, Jenkins ML, Holtzman SG, Cucinell SA, and Dayton PG (1974) Metabolism and disposition of methylphenidate-14C: studies in man and animals. *J Pharmacol Exp Ther* 191**:**535-547.

Hungund BL, Perel JM, Hurwic MJ, Sverd J, and Winsberg BG (1979) Pharmacokinetics of methylphenidate in hyperkinetic children. *Br J Clin Pharmacol* 8**:**571-576.

Hysek CM, Simmler LD, Schillinger N, Meyer N, Schmid Y, Donzelli M, Grouzmann E, and Liechti ME (2014) Pharmacokinetic and pharmacodynamic effects of methylphenidate and MDMA administered alone or in combination. *Int J Neuropsychopharmacol* 17**:**371-381.

Koehm M, Kauert GF, and Toennes SW (2010) Influence of ethanol on the pharmacokinetics of methylphenidate's metabolites ritalinic acid and ethylphenidate. *Arzneimittelforschung* 60**:**238-244.

Meyer MC, Straughn AB, Jarvi EJ, Patrick KS, Pelsor FR, Williams RL, Patnaik R, Chen ML, and Shah VP (2000) Bioequivalence of methylphenidate immediate-release tablets using a replicated study design to characterize intrasubject variability. *Pharm Res* 17**:**381-384.

Midha KK, McKay G, Rawson MJ, Korchinski ED, and Hubbard JW (2001) Effects of food on the pharmacokinetics of methylphenidate. *Pharm Res* 18**:**1185-1189.

Ohlsson A, Lindgren JE, Andersson S, Agurell S, Gillespie H, and Hollister LE (1986) Single-dose kinetics of deuterium-labelled cannabidiol in man after smoking and intravenous administration. *Biomed Environ Mass Spectrom* 13**:**77-83.

Parasrampuria DA, Schoedel KA, Schuller R, Gu J, Ciccone P, Silber SA, and Sellers EM (2007) Assessment of pharmacokinetics and pharmacodynamic effects related to abuse potential of a unique oral osmotic-controlled extended-release methylphenidate formulation in humans. *J Clin Pharmacol* 47**:**1476-1488.

Patrick KS, Straughn AB, Jarvi EJ, Breese GR, and Meyer MC (1989) The absorption of sustained-release methylphenidate formulations compared to an immediate-release formulation. *Biopharm Drug Dispos* 10**:**165-171.

Patrick KS, Straughn AB, Minhinnett RR, Yeatts SD, Herrin AE, DeVane CL, Malcolm R, Janis GC, and Markowitz JS (2007) Influence of ethanol and gender on methylphenidate pharmacokinetics and pharmacodynamics. *Clin Pharmacol Ther* 81**:**346-353.

Patrick KS, Straughn AB, Reeves OT, 3rd, Bernstein H, Bell GH, Anderson ER, and Malcolm RJ (2013) Differential influences of ethanol on early exposure to racemic methylphenidate compared with dexmethylphenidate in humans. *Drug Metab Dispos* 41**:**197-205.

Spencer TJ, Biederman J, Ciccone PE, Madras BK, Dougherty DD, Bonab AA, Livni E, Parasrampuria DA, and Fischman AJ (2006) PET study examining pharmacokinetics, detection and likeability, and dopamine transporter receptor occupancy of short- and long-acting oral methylphenidate. *Am J Psychiatry* 163**:**387-395.

Spencer TJ, Biederman J, Martin JM, Moorehead TM, Mirto T, Clarke A, Batchelder H, and Faraone SV (2012) Importance of pharmacokinetic profile and timing of coadministration of short- and long-acting formulations of methylphenidate on patterns of subjective responses and abuse potential. *Postgrad Med* 124**:**166-173.

Srinivas NR, Hubbard JW, Korchinski ED, and Midha KK (1993) Enantioselective pharmacokinetics of dl-threo-methylphenidate in humans. *Pharm Res* 10**:**14-21.

Stage C, Jurgens G, Guski LS, Thomsen R, Bjerre D, Ferrero-Miliani L, Lyauk YK, Rasmussen HB, Dalhoff K, and Consortium I (2017) The impact of CES1 genotypes on the pharmacokinetics of methylphenidate in healthy Danish subjects. *Br J Clin Pharmacol* 83**:**1506-1514.

Stott C, White L, Wright S, Wilbraham D, and Guy G (2013) A Phase I, open-label, randomized, crossover study in three parallel groups to evaluate the effect of Rifampicin, Ketoconazole, and Omeprazole on the pharmacokinetics of THC/CBD oromucosal spray in healthy volunteers. *Springerplus* 2**:**236.

Sun Z, Murry DJ, Sanghani SP, Davis WI, Kedishvili NY, Zou Q, Hurley TD, and Bosron WF (2004) Methylphenidate is stereoselectively hydrolyzed by human carboxylesterase CES1A1. *J Pharmacol Exp Ther* 310**:**469-476.

Taylor L, Crockett J, Tayo B, and Morrison G (2019) A Phase 1, Open-Label, Parallel-Group, Single-Dose Trial of the Pharmacokinetics and Safety of Cannabidiol (CBD) in Subjects With Mild to Severe Hepatic Impairment. *J Clin Pharmacol* 59**:**1110-1119.

Taylor L, Gidal B, Blakey G, Tayo B, and Morrison G (2018) A Phase I, Randomized, Double-Blind, Placebo-Controlled, Single Ascending Dose, Multiple Dose, and Food Effect Trial of the Safety, Tolerability and Pharmacokinetics of Highly Purified Cannabidiol in Healthy Subjects. *CNS Drugs* 32**:**1053-1067.

Tayo B, Taylor L, Sahebkar F, and Morrison G (2020) A Phase I, Open-Label, Parallel-Group, Single-Dose Trial of the Pharmacokinetics, Safety, and Tolerability of Cannabidiol in Subjects with Mild to Severe Renal Impairment. *Clin Pharmacokinet* 59**:**747-755.

Teo SK, Scheffler MR, Wu A, Stirling DI, Thomas SD, Stypinski D, and Khetani VD (2004) A single-dose, two-way crossover, bioequivalence study of dexmethylphenidate HCl with and without food in healthy subjects. *J Clin Pharmacol* 44**:**173-178.

Wang Y, Lee L, Somma R, Thompson G, Bakhtiar R, Lee J, Rekhi GS, Lau H, Sedek G, and Hossain M (2004) In vitro dissolution and in vivo oral absorption of methylphenidate from a bimodal release formulation in healthy volunteers. *Biopharm Drug Dispos* 25**:**91-98.

Wong YN, King SP, Laughton WB, McCormick GC, and Grebow PE (1998) Single-dose pharmacokinetics of modafinil and methylphenidate given alone or in combination in healthy male volunteers. *J Clin Pharmacol* 38**:**276-282.